NATIONAL ADVISORY COMMITTEE FOR AERONAUTICS

TECHNICAL NOTE 3859

COMPARISON OF FLIGHT AND WIND-TUNNEL MEASUREMENTS OF HIGH-SPEED-AIRPLANE STABILITY AND CONTROL CHARACTERISTICS

By Walter C. Williams, Hubert M. Drake, and Jack Fischel

High-Speed Flight Station
Edwards, California

NACA
Washington
August 1956

NATIONAL ADVISORY COMMITTEE FOR AERONAUTI(

TECHNICAL NOTE 3859

COMPARISON OF FLIGHT AND WIND-TUNNEL MEASUREMENTS OF HIGH-SPEED-AIRPLANE STABILITY AND CONTROL CHARACTERISTICS[1]

By Walter C. Williams, Hubert M. Drake, and Jack Fischel

SUMMARY

Comparisons of wind-tunnel and flight-measured values of stability and control characteristics are of considerable interest to the designer, since the wind-tunnel method of testing is one of the prime sources upon which estimates of the characteristics of a new configuration are based. In this paper comparisons are made of some of the more important stability and control characteristics of three swept-wing airplanes as measured in flight and in wind tunnels. Wind-tunnel data from high-speed closed-throat tunnels, a slotted-throat transonic tunnel, and a supersonic tunnel are used.

The comparisons show that, generally speaking, the wind tunnels predict all trends of characteristics reasonably well. There are, however, differences in exact values of parameters, which could be attributed somewhat to differences in the model caused by the method of support. The small size of the models may have some effect on measurements of flap effectiveness. When nonlinearities in derivatives occur during wind-tunnel tests, additional data should be obtained in the region of the nonlinearities in order to predict more accurately the flight characteristics. Also, nonlinearities in static derivatives must be analyzed on the basis of dynamic motions of the airplane. Aeroelastic corrections must be made to the wind-tunnel data for models of airplanes which have thin surfaces and are to be flown at high dynamic pressures. Inlet effects can exert an influence on the characteristics, depending upon air requirements of the engine and location of the inlets.

---

[1]The information in this report was also contained in a paper by the same authors entitled: "Some Correlations of Flight-Measured and Wind-Tunnel Measured Stability and Control Characteristics of High-Speed Airplanes." The latter was presented to the Wind Tunnel and Model Testing Panel of the NATO Advisory Group for Aeronautical Research and Development at the meeting in Brussels, Belgium, August 27-31, 1956.

INTRODUCTION

One of the principal tools of the aircraft designer in predicting the stability and control characteristics of a new airplane is the use of models tested in wind tunnels. There is, of course, the question whether the model results accurately predict characteristics of the airplane in free flight or, in other words, the question of the degree of correlation between the two results. This problem has received considerable attention. Most of this work, reference 1 for example, has been performed at subsonic speeds and indicates that, in general, good correlation can be obtained when the model accurately represents the actual aircraft, and the tests, both flight and wind tunnel, are carefully performed.

Some work has been reported on the correlation between the wind-tunnel and flight-measured stability characteristics in the transonic speed regime (ref. 2). Correlations of transonic and supersonic results are currently of particular interest in view of the availability of wind tunnels capable of testing through the transonic speed range. Problems of correlations in this speed range are complicated by the compromises imposed on the model by the mounting system; for example, sting supports require that the rear end of the fuselage be altered. It is also necessary in high-speed tunnels to utilize much smaller models than were possible in the low-speed tunnels. The purpose of this paper is to present some correlations of several of the more important flight-measured and wind-tunnel-measured stability and control characteristics of high-speed airplanes.

SYMBOLS

b	wing span, ft
C_{l_p}	damping-in-roll coefficient, per radian
C_{l_δ}	rolling-moment coefficient per degree aileron deflection
C_m	pitching-moment coefficient
$C_{m_{C_L}}$	static margin, percent mean aerodynamic chord
$\Delta C_{m_{C_L}}$	$\left(C_{m_{C_L}}\right)_{WT} - \left(C_{m_{C_L}}\right)_F$

$C_{m_{i_t}}$	pitching-moment coefficient per degree stabilizer deflection
$C_{m_{\dot{\theta}}} + C_{m_{\dot{\alpha}}}$	damping coefficient in pitch
C_N	normal-force coefficient
C_{N_α}	normal-force-curve slope, per deg
C_{n_β}	directional stability parameter, per radian
$\bar{c}$	wing mean aerodynamic chord, ft
I_Y	airplane moment of inertia in pitch, slug-ft^2
i_t	stabilizer angle, negative when stabilizer leading edge down, deg
Δi_t	$(i_t)_{WT} - (i_t)_F$
M	Mach number
m_a	mass rate of air intake, slugs/sec
$\frac{pb}{2V}/\delta$	wing-tip helix angle per degree aileron deflection, radians/deg
q	dynamic pressure, lb/sq ft
S	airplane wing area, sq ft
V	true airspeed, ft/sec
x_a	distance from airplane center of gravity to air intake of jet engine, ft
α	angle of attack, deg
$\dot{\theta}$	pitching velocity, radians/sec
$\ddot{\theta}$	pitching acceleration, radians/sec^2
τ	relative elevator-stabilizer effectiveness

Subscripts:

1	initial condition at start of maneuver
F	flight
WT	wind tunnel

AIRPLANES AND TESTS

Three swept-wing airplanes are considered in this study. All are single engine, fighter-type airplanes with a sweep range from 35° to 60°. Much of the flight data were obtained at an altitude of 40,000 feet with some of the supersonic data extending to altitudes as high as 60,000 feet. The overall Reynolds number variation was from 8 million to 19.5 million. The flight data were obtained with power on, involving for the most part between 90 percent and 100 percent available thrust.

The wind-tunnel tests for these airplanes were performed in the following NACA wind tunnels:

Langley 8-foot transonic tunnel
Langley 8-foot high-speed tunnel
Langley high-speed 7- by 10-foot tunnel
Langley 4- by 4-foot supersonic pressure tunnel

All models were sting supported and the forces were measured by internally mounted strain-gage balances. The Reynolds number ranges of the tests varied from 1.9 million to 3.6 million. The model tests were made with no power simulation and the inlets were faired, except for airplane A which employed an open duct. There were differences between the models and the actual airplanes in most cases. These differences and the model scales are as follows:

Airplane A (1/11-scale model)
8-foot transonic tunnel
High-speed 7- by 10-foot tunnel

(1) The wind-tunnel model incorporated an enlargement at the rear end of the fuselage to accomodate the sting support.

(2) The wind-tunnel model exposed-horizontal-tail area was maintained, and an increased tail span therefore resulted.

The plan form differences for airplane A are shown in figure 1.

Airplane B (1/16-scale model)
8-foot high-speed tunnel (closed throat)
8-foot transonic tunnel
7- by 10-foot high-speed tunnel (closed throat)
4- by 4-foot supersonic pressure tunnel

(1) The wind-tunnel model incorporated an enlargement at the rear end of the fuselage to accommodate the sting support.

(2) The wind-tunnel model incorporated constant-percentage-chord wing sections, whereas the airplane wing incorporated similar root sections but thicker tip sections than the wind-tunnel model. In addition, during tests in the 8-foot high-speed (closed throat) tunnel and the 4- by 4-foot supersonic pressure tunnel, the model was tested without a cockpit canopy.

Airplane C (1/14-scale model)
8-foot transonic tunnel
4- by 4-foot supersonic pressure tunnel

RESULTS AND DISCUSSION

One of the prime considerations in the measurement of airplane characteristics is the lift-curve slope of the airplane. A comparison of the variation of normal-force coefficient with angle of attack for airplane A, as measured in flight and in the 8-foot transonic tunnel at Mach numbers of 0.76 and 0.91, is shown in the upper part of figure 2. The data are for trimmed conditions. As can be seen in this figure, the correlation is reasonably good in the linear range. At angles of attack above peak lift or above the break in the curve that are indicative of separated flow, there are discrepancies. The lower part of this figure shows the variation with Mach number of the ratio of flight-determined to wind-tunnel-determined normal-force-coefficient slope for airplanes A and B. These slopes were taken at a normal-force coefficient close to the value for level flight. As can be seen, the results are within 10 percent of each other, with the flight-measured values being generally higher. The transonic data up to $M = 1.15$ were obtained from the 8-foot transonic tunnel, the data at $M = 1.2$ from the 8-foot high-speed tunnel, and the higher Mach number data were obtained from the 4- by 4-foot supersonic pressure tunnel.

Determination of the static margin is important in establishing the necessary center-of-gravity position for a configuration. The variation of static margin $C_{m_{C_L}}$ with Mach number is shown in figure 3 for airplane A, as measured in the 8-foot transonic tunnel, and as measured in

flight from pulse disturbances. The data are referenced to the same center-of-gravity position. This figure shows that similar variations of static margin with Mach number are exhibited in the two sets of data. The flight data, however, show a value of static margin consistently higher by about 3 percent. It is believed that differences between the model and the airplane at the rear of the fuselage and horizontal-tail configurations (fig. 1) could account for these discrepancies. The lower part of figure 3 shows the incremental difference in static margin $\Delta C_{m_{C_L}}$ between the data from the two test mediums for airplanes A and B at normal-force coefficients for level flight. As stated previously, the data for airplane A exhibit a constant difference of about 3 percent. The flight values for airplane B are about 5 percent higher than the data from the closed-throat tunnel up to a Mach number of about 0.85. Above this Mach number the difference decreases, and at a Mach number of about 0.95 the wind-tunnel data show about 5 percent greater static margin than that shown by the flight tests. This variation between Mach numbers of 0.85 and 0.95 is believed to be caused by choking effects in the closed-throat tunnel. The results from the transonic tunnel (slotted throat) are similar to those from the closed-throat tunnel up to a Mach number of 0.85. Above this Mach number the difference in static margin varies somewhat, but throughout the Mach number range of this test the flight data show higher static margins by 1 to 5 percent. The higher supersonic data for airplane B show similar increments in static margin.

In addition to checking the levels of longitudinal stability, it is important with high-speed configurations to establish the variations of stability with angle of attack in order to explore for the existence of nonlinearities which may lead to an undesirable characteristic, such as pitch-up. Typical variations of pitching moment with angle of attack for airplane A, as measured in flight and in the 8-foot transonic tunnel at Mach numbers of 0.76 and 0.91, are shown in figure 4. The flight data for the wing-fuselage pitching-moment coefficient (tail off) were obtained from measurements of horizontal-tail loads. It should be noted that the tail loads were measured by strain gages mounted at the roots of the horizontal tail and represent only the panel loading without carry-over to the fuselage. These measurements are in error, therefore, by the unknown amount of the carry-over. The overall airplane pitching moment was obtained primarily from flight measurement of the variation of stabilizer angle with angle of attack in accelerated maneuvers, turns, and pull-ups made at constant Mach number. These variations of stabilizer angle with angle of attack were corrected for pitching acceleration by the expression

$$(\Delta i_t)_{\ddot{\theta}} = \frac{\frac{I_Y \ddot{\theta}}{q S \bar{c}}}{C_{m_{i_t}}}$$

The corrected data were converted to pitching-moment coefficient by the following simplified expression, which includes the effects of pitch damping

$$C_m = - C_{m_{i_t}}\left(i_t - i_{t_1}\right) - \frac{\left(C_{m_{\dot{\theta}}} + C_{m_{\dot{\alpha}}}\right)\dot{\theta}\bar{c}}{2V}$$

In these calculations the pitching-moment coefficient due to stabilizer deflection $C_{m_{i_t}}$ was assumed constant over the angle-of-attack range. The data of figure 4 show that the pitching-moment curves from the two sources are generally similar. At both Mach numbers the comparison between flight and wind-tunnel results yielded a difference in the angle of attack for trim. At a Mach number of 0.76, however, the nonlinearities occur in the tunnel data at lower angles of attack and the data do not exhibit the large dip in the curve that is shown for the flight results. This difference could possibly be accounted for by the lack of sufficient wind-tunnel test points to define such a variation, since there is no wind-tunnel test point between an angle of attack of 10° and 12°, where such a dip might be expected to appear if it existed in the wind-tunnel results. The data at a Mach number of 0.91 are considered to be reasonably similar, both with tail off and tail on. It should be pointed out that inspection of the shape of the pitching-moment curves is not sufficient to determine whether or not a pitch-up problem exists. It has been found that pitch-up can be a problem even with airplanes having neutral stability or even slightly positive stability in the nonlinear region. The degree of stability above the pitch-up is also important. In order to evaluate pitch-up, it is necessary to make calculations of the motions of the airplane in dynamic maneuvers by using assumed arbitrary pilot control inputs (ref. 3). It is believed that these wind-tunnel data represent the flight case closely enough for such calculations to be of value in predicting the maneuvering characteristics of the airplane.

Another important longitudinal characteristic is the variation with Mach number of the longitudinal control deflection required for level flight. Data of this type are shown in figure 5. The upper portion of the figure shows the variation with Mach number of the stabilizer deflection for trim for airplane A as measured in flight and in the 8-foot transonic tunnel. As can be seen, the variations are generally similar for the two tests, with flight-measured data showing a larger change in stabilizer deflection required above a Mach number of 0.90 than shown by the wind-tunnel data. In the lower portion of the figure where the differences between flight and wind-tunnel measurement are shown for airplanes A and B, it can be seen that the difference between flight and wind-tunnel trim values exceeds 1° of stabilizer travel only at a Mach number of 0.98 for airplane A. Over most of the range there is less than 0.5° difference in stabilizer deflection required for trim.

Although elevator control on high-speed airplanes is being replaced by all-movable or one-piece horizontal tails, it appears that flap-type rudders and ailerons may continue to be used. Some comparisons of measured values of relative elevator-stabilizer effectiveness are shown in figure 6. The upper portion of this figure compares the variations of relative elevator-stabilizer effectiveness τ with Mach number as measured in flight and in the wind tunnel. This figure shows that there is an appreciable difference between the flight and wind-tunnel data, particularly above a Mach number of 0.9 where a much larger decrease in relative elevator-stabilizer effectiveness was measured in flight than in the wind tunnel. Data are shown in the lower part of figure 6 on the basis of the ratio of flight-measured to wind-tunnel-measured values of τ for airplanes A and B. Although the values of τ from the two sources are within 10 percent of one another below a Mach number of 0.8, the differences between flight and wind-tunnel values at transonic speeds are as high as ±25 percent. Somewhat better agreement is shown for the supersonic data than for the transonic data. At a Mach number of 1.6 the data for airplane B are in perfect agreement, which may be fortuitous. The small size of elevators used on wind-tunnel models such as these make the measurement difficult.

Additional flap-effectiveness data are shown in figure 7 in which some aileron effectiveness information for airplane B is shown. In the upper part of this figure the ratio of flight-measured to wind-tunnel-measured values of $\frac{pb}{2V}\Big/\delta$ is shown as a function of Mach number. The flight-measured values are generally lower than the wind-tunnel values, reaching only 70 percent of the wind-tunnel values at Mach numbers above 0.90. This difference is understandable when it is considered that the wind-tunnel data for rolling-moment coefficient were obtained under static conditions and the aileron effectiveness was calculated, on the assumption of freedom only in roll, by the following expression

$$\frac{pb}{2V}\Big/\delta = \frac{C_{l_\delta}}{C_{l_p}}$$

In addition, it should be noted that the outboard wing sections of the airplane were thicker than those of the wind-tunnel model, as discussed previously. Moreover, inasmuch as the damping-in-roll coefficient C_{l_p} was not measured for this model, values of C_{l_p} used in the present calculations were based on those measured for almost comparable wing configurations. Better correlation would probably be obtained if the effectiveness were calculated by assuming freedom in roll, yaw, and sideslip. In some cases it may be necessary to include freedom in pitch and angle of attack as well. The usual testing technique is to obtain the flight data in rudder-fixed aileron rolls where the airplane experiences motions about all axes. Aeroelasticity is not believed to be an

important factor in the difference between results, because the flight-test results did not show a significant effect of dynamic pressure within the range tested. The lower part of figure 7 shows the variation of aileron effectiveness with Mach number for the two tests with the data arbitrarily normalized to the value of effectiveness existing at $M = 0.6$. The data show close agreement between the flight- and wind-tunnel-measured variation of aileron effectiveness with Mach number. It appears, therefore, that if the level of aileron effectiveness could be determined accurately from model tests at low speeds, it might be expected that the wind-tunnel tests could accurately predict the decrease in effectiveness with increasing Mach number.

Static directional stability of a new configuration is of importance to the designer since it is one of the more important parameters used in determining airplane behavior under dynamic as well as static lateral conditions. It has been found that many of the high-speed configurations exhibit large changes in directional stability with angle of attack. Typical data for airplane A are shown in the upper portion of figure 8, where the static directional stability derivative C_{n_β} is plotted as a function of angle of attack. These data were obtained in the 7- by 10-foot tunnel at a Mach number of 0.70. There are no comparable flight data for this case because of the difficulty of measurement in flight. As can be seen in this figure, the directional stability parameter becomes zero at an angle of attack of about 18°. From data such as these, the variation with Mach number of the angle of attack at which C_{n_β} is zero was determined. This boundary is plotted on the lower part of this figure. Also shown are points which represent the combinations of angle of attack and Mach number at which directional divergences have occurred in flight. It should be noted that, for any given Mach number, divergences occurred at angles of attack both less than and greater than that required for zero directional stability. It appears that, as in the case of pitch-up, dynamic analysis of the airplane motions is required in order to assess the problem.

Another variation of directional stability of concern to designers is that which occurs with changes in Mach number. Figure 9 relates the variation of C_{n_β} with Mach number as measured in the wind tunnel to that measured in flight for airplane C. As can be seen, there are large discrepancies amounting to as much as 50 percent difference between the basic wind-tunnel data and the flight-measured values. In the previous cases shown, relatively thick airfoil sections were used on the empennage and the dynamic pressure for the tests was relatively low, less than 400 pounds per square foot. In the present case the vertical-tail thickness was about half that of the other airplanes, and the maximum dynamic pressure experienced was of the order of 850 pounds per square foot. Aeroelastic effects were found to be of importance. When the wind-tunnel data were corrected for aeroelastic effects, primarily bending and

twisting of the vertical tail, the agreement between the data from the two sources was improved but differences as high as 20 percent still remained. Because airplane C has a large jet engine and a nose inlet, the wind-tunnel data were then corrected for inlet effects by the expression

$$\Delta C_{n_\beta} = - \frac{m_a V x_a}{qSb}$$

As can be seen, when this correction was made, the wind-tunnel tests gave values of the directional stability parameter that were within 10 percent of the flight values throughout the Mach number range.

CONCLUDING REMARKS

Comparisons of wind-tunnel and flight-measured stability and control characteristics showed that the wind-tunnel data predicted all trends of characteristics reasonably well. Discrepancies were found in exact values, which may be attributed to differences in the models caused by mounting considerations and, in the case of control effectivenesses, to the small size of the models. Where nonlinearities in derivatives occur during wind-tunnel testing, it may be necessary to obtain additional data points in the region of the nonlinearities in order to predict more accurately the flight characteristics. Nonlinearities in static derivatives should be analyzed under dynamic conditions. Aeroelasticity must be considered in evaluating data dealing with thin airfoils and high dynamic pressures. Inlet effects can be important, depending on the size of the engine and the location of the inlets.

High-Speed Flight Station,
National Advisory Committee for Aeronautics,
Edwards, Calif., August 21, 1956.

REFERENCES

1. Kayten, Gerald G., and Koven, William: Comparison of Wind-Tunnel and Flight Measurements of Stability and Control Characteristics of a Douglas A-26 Airplane. NACA Rep. 816, 1945. (Formerly NACA ARR L5H11a.)

2. Duddy, R. R.: Some Comparisons Between Wind Tunnel Model and Flight Test Results on Aircraft at High Angles of Attack. Papers Presented at the Joint Session of the Flight Test Techniques and Wind Tunnel and Model Testing Panels, Ottawa, Canada. AG18/P8, AGARD, North Atlantic Treaty Organization, June 1955, pp. 107-125.

3. Stone, Ralph W., Jr.: Interpretation of Wind-Tunnel Data in Terms of Dynamic Behavior of Aircraft at High Angles of Attack. Papers Presented at the Joint Session of the Flight Test Techniques and Wind Tunnel and Model Testing Panels, Ottawa, Canada. AG18/P8, AGARD, North Atlantic Treaty Organization, June 1955, pp. 24-50.

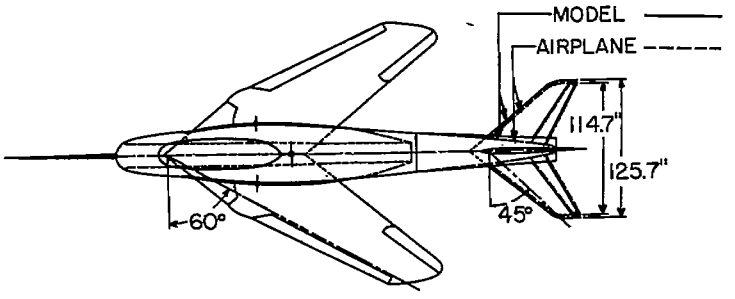

Figure 1.- Plan form of airplane A.

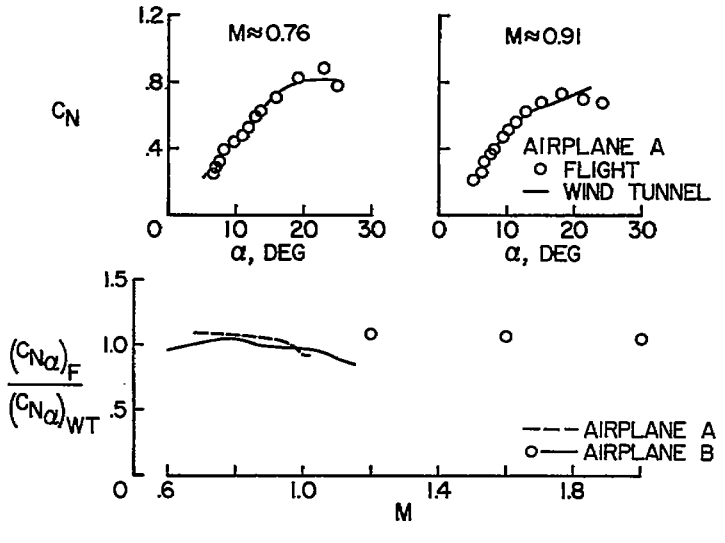

Figure 2.- Correlation of flight and wind-tunnel lift characteristics for airplanes A and B.

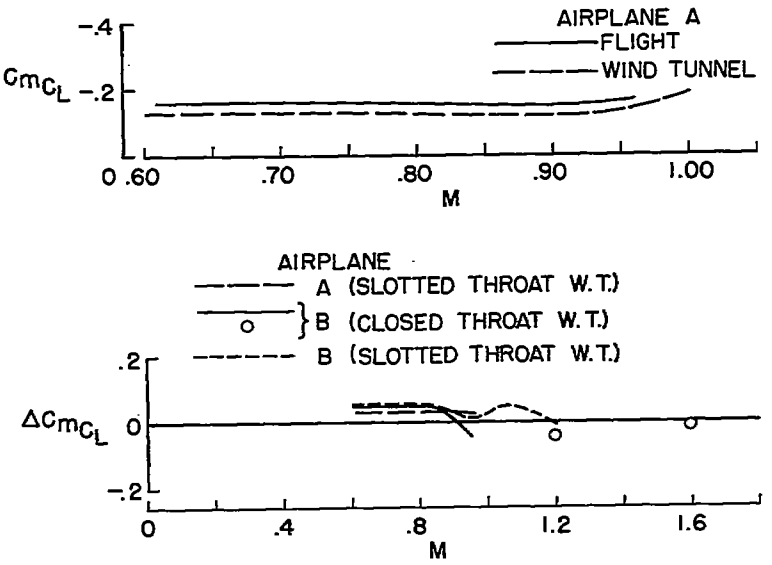

Figure 3.- Comparison of static margin determined in flight and wind-tunnel tests for airplanes A and B.

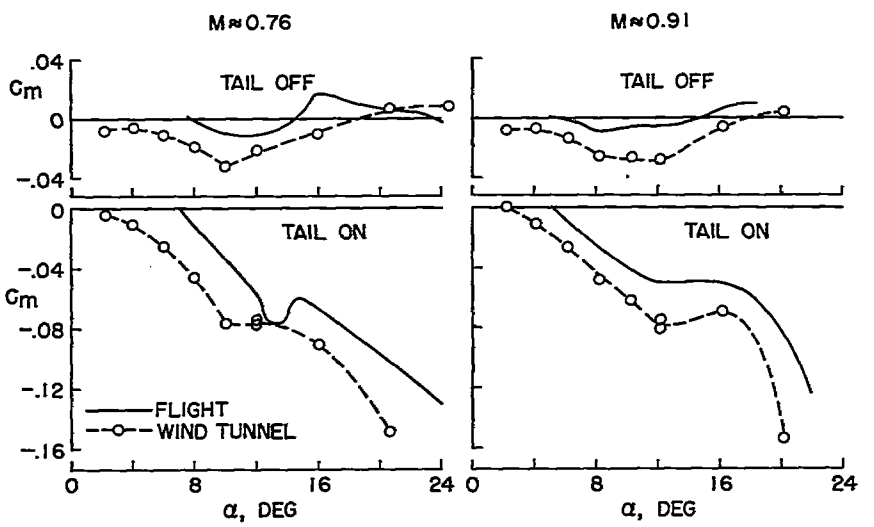

(a) M ≈ 0.76. (b) M ≈ 0.91.

Figure 4.- Flight and wind-tunnel pitching-moment characteristics for airplane A with and without horizontal tail.

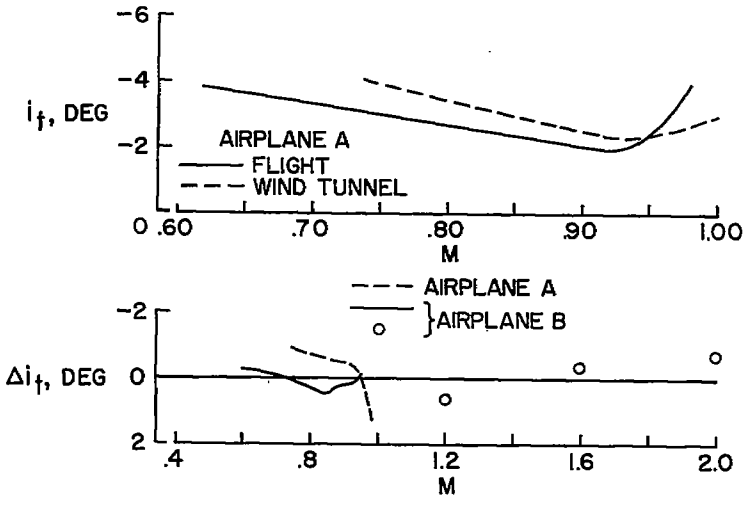

Figure 5.- Trim characteristics determined in flight and wind-tunnel tests for airplanes A and B.

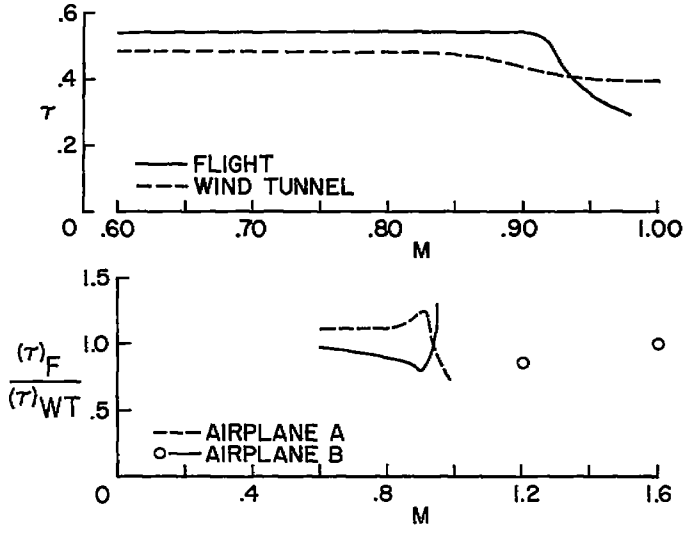

Figure 6.- Relative elevator-stabilizer effectiveness determined in flight and wind-tunnel tests for airplanes A and B.

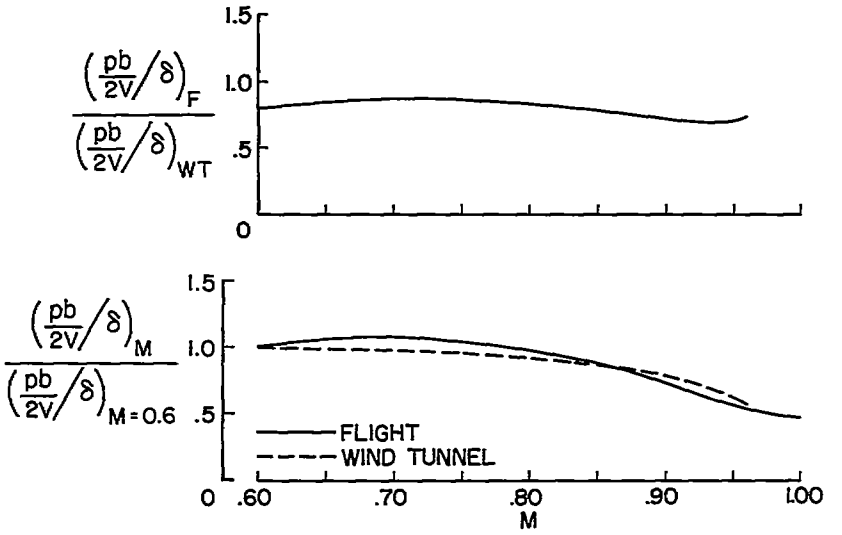

Figure 7.- Aileron effectiveness characteristics determined in flight and wind tunnel for airplane B.

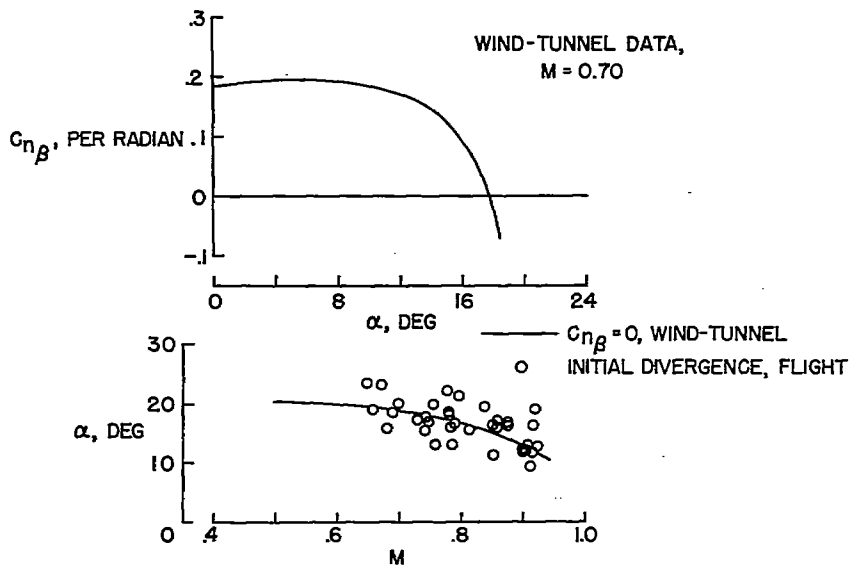

Figure 8.- Comparison of flight and wind-tunnel directional-instability characteristics. Airplane A.

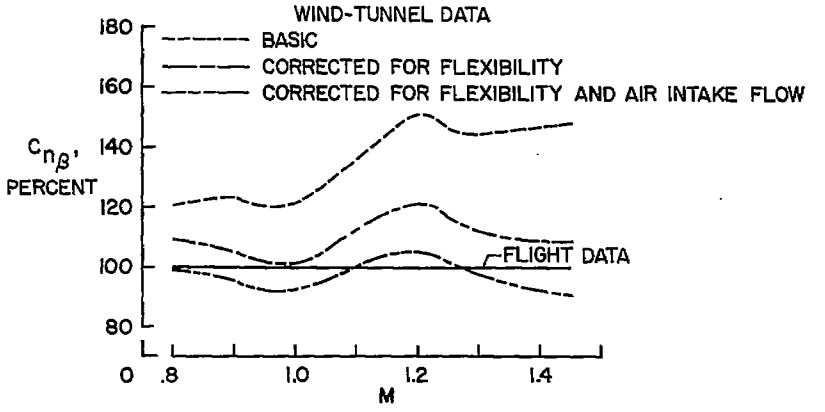

Figure 9.- Comparison of flight and wind-tunnel directional-stability characteristics. Airplane C.